# Nuclear transparency of the charged hadrons produced in the electronuclear reaction

Swapan Das *

*Nuclear Physics Division, Bhabha Atomic Research Centre, Trombay, Mumbai 400085, India*
*and Homi Bhabha National Institute, Anushakti Nagar, Mumbai 400094, India*

(Received 30 September 2021; accepted 2 March 2022; published 25 March 2022)

The nuclear transparency of charged hadrons produced in the $(e, e')$ reaction on nuclei has been calculated using the Glauber model for the nuclear reaction. The color transparency (CT) of produced hadrons and the short-range correlation (SRC) of nucleons in the nucleus have been incorporated in the Glauber model to investigate their effects on nuclear transparency. The calculated results for the proton and pion are compared with the data.

DOI: 10.1103/PhysRevC.105.035204

## I. INTRODUCTION

The hadron-nucleus cross section is less than that in the plane-wave impulse approximation (PWIA) because the initial and/or final state interaction(s) of a hadron with the nucleus are neglected in PWIA. This phenomenon is characterized by the nuclear transparency $T_A$, defined [1] as

$$T_A = \frac{\sigma_{hA}}{\sigma_{hA(\mathrm{PWIA})}}, \tag{1}$$

where $\sigma_{hA}$ represents the hadron-nucleus cross section.

The transverse size $d_\perp$ of the hadron produced in a nucleus due to the spacelike high momentum transfer $Q^2$ is reduced as $d_\perp \sim 1/Q$ [1,2]. The reduced (in size) hadron is referred as a pointlike configuration (PLC) [1]. According to quantum chromodynamics, a color neutral PLC has reduced interaction with the nucleon in a nucleus because the sum of its gluon emission amplitudes cancels[1,3]. The PLC expands to the size of a physical hadron, as it moves up to a length ($\approx$1 fm) called hadron formation length $l_h$ [1,4]:

$$l_h = \frac{2k_h}{\Delta M^2}, \tag{2}$$

where $k_h$ is the momentum of the hadron in the laboratory frame. $\Delta M^2$ is related to the mass difference between the hadronic states originating due to the (anti)quarks' fluctuation in the PLC. The interaction of the PLC with the nucleon in a nucleus increases, as its size enlarges during its passage through the nucleus. The decrease in the hadron-nucleon cross section in a nucleus, as explained by the Glauber model [5], leads to the increase in the hadron-nucleus cross section. Therefore, the transparency $T_A$ in Eq. (1) of the hadron rises. The enhancement in $T_A$ due to the above phenomenon is referred as color transparency (CT) of the hadron. The physics of CT for hadrons has been discussed elaborately in Refs. [3,6].

Experiments on the nuclear transparency in $A(p, pp)$ reactions were done at Brookhaven National Laboratory (BNL) [7] to search for the CT of the proton ($p$CT). The measured spectra for nuclei show a peak in the energy distribution that could not be reproduced by the results calculated considering the $p$CT in the Glauber model [8]. The data can be understood by other mechanisms (e.g., see Brodsky *et al.* [9] and Ralston *et al.* [10]) for the $pp$ scattering in a nucleus. The $p$CT is also not seen in the $A(e, e'p)$ experiment done at the Stanford Linear Accelerator Center (SLAC) [11] and at Jefferson Laboratory (JLab) [12] for the photon virtuality $Q^2 = 0.64$–$8.1$ GeV$^2$. The transparency measured in the $(e, e'p)$ reaction on $^{12}$C for $8 \leqslant Q^2 \leqslant 14.2$ GeV$^2$ [13] at the upgraded JLab facility agrees with the previous observations [11,12]. The calculated proton transparency in this reaction [14,15]) corroborates the experimental finding.

Since the meson is a bound state of two quarks (i.e., quark-antiquark) the PLC formation of it can be more probable than that of the baryon, a three-quark ($qqq$) system. The color transparency is unambiguously reported from Fermi National Accelerator Laboratory (FNAL) [16] in the experiment of the nuclear diffractive dissociation of the pion (of 500 GeV/$c$) to dijets. The color transparency is also illustrated in $\pi^-$ meson photoproduction [17] and $\rho^0$ meson electroproduction (from nuclei) experiments [18]. There exist calculated results for the $\rho$-meson color transparency in the energy region available at JLab [1,19].

The nuclear transparency of the $\pi^+$ meson produced in the $A(e, e')$ process was measured at JLab for $Q^2 = 1.1$–$4.7$ GeV$^2$ [20]. The data have been understood by using the pionic color transparency ($\pi$CT) [4]. Larson *et al.* [21] described the momentum dependence of $\pi$CT in the above reaction. The $\pi$CT in the electronuclear reaction has also been studied by Cosyn *et al.* [22] and Kaskulov *et al.* [23] for the energy region available at JLab [20]. Larionov *et al.* [4] estimated the $\pi$CT in the $(\pi^-, l^+l^-)$ reaction on nuclei for $p_\pi = 5$–$20$ GeV/$c$, which can be measured using the forthcoming facilities at the Japan Proton Accelerator Research Complex (J-PARC) [24]. This reaction provides information complementary to that obtained from the $A(\gamma^*, \pi)$ reaction. Miller and Strikman [25] illustrated large CT in the pionic knockout of protons

* swapand@barc.gov.in

 

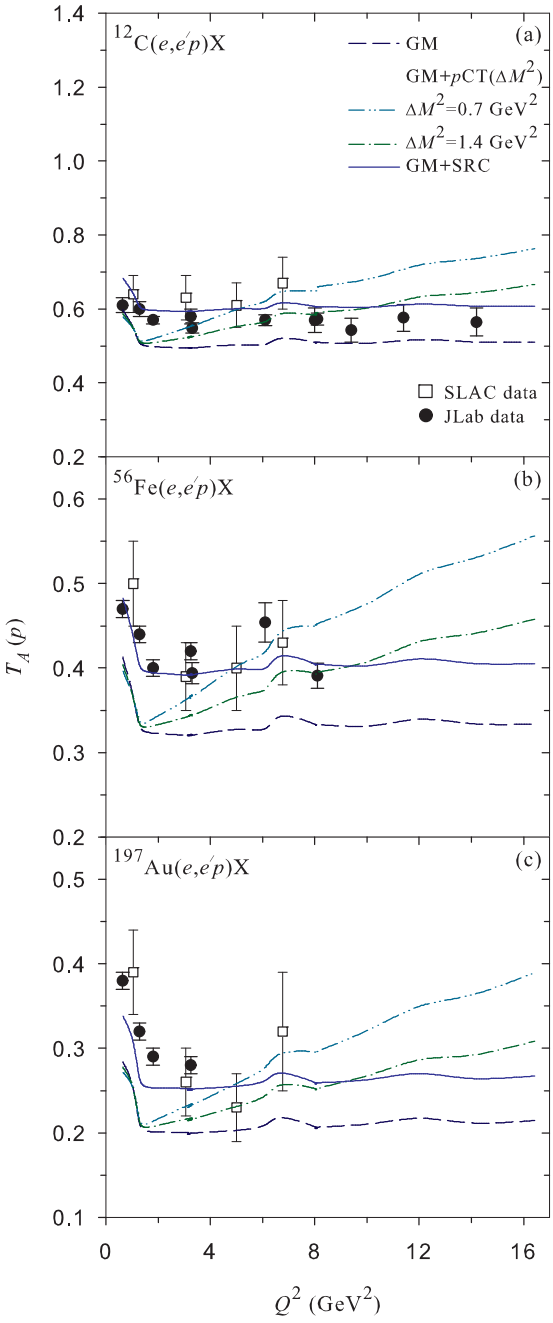


FIG. 1. The calculated nuclear transparency of the proton $T_A(p)$ vs photon virtuality $Q^2$. The medium-dashed curves denote $T_A(p)$ evaluated using the Glauber model (GM). The dot-dot-dashed and dot-dashed curves illustrate the proton color transparency ($p$CT) for two different values of $\Delta M^2$ used in the Glauber model (GM + $p$CT); see text. The solid curves arise due to the inclusion of short-range correlation (SRC) in the Glauber model (GM + SRC). The data are taken from Refs. [11–13].

off nuclei at the energy 200 GeV available at the CERN COMPASS experiment.

The enhancement in $T_A$ due to $\sigma_{hA}$ in Eq. (1) can also occur because of the short-range correlation (SRC) of nucleons in

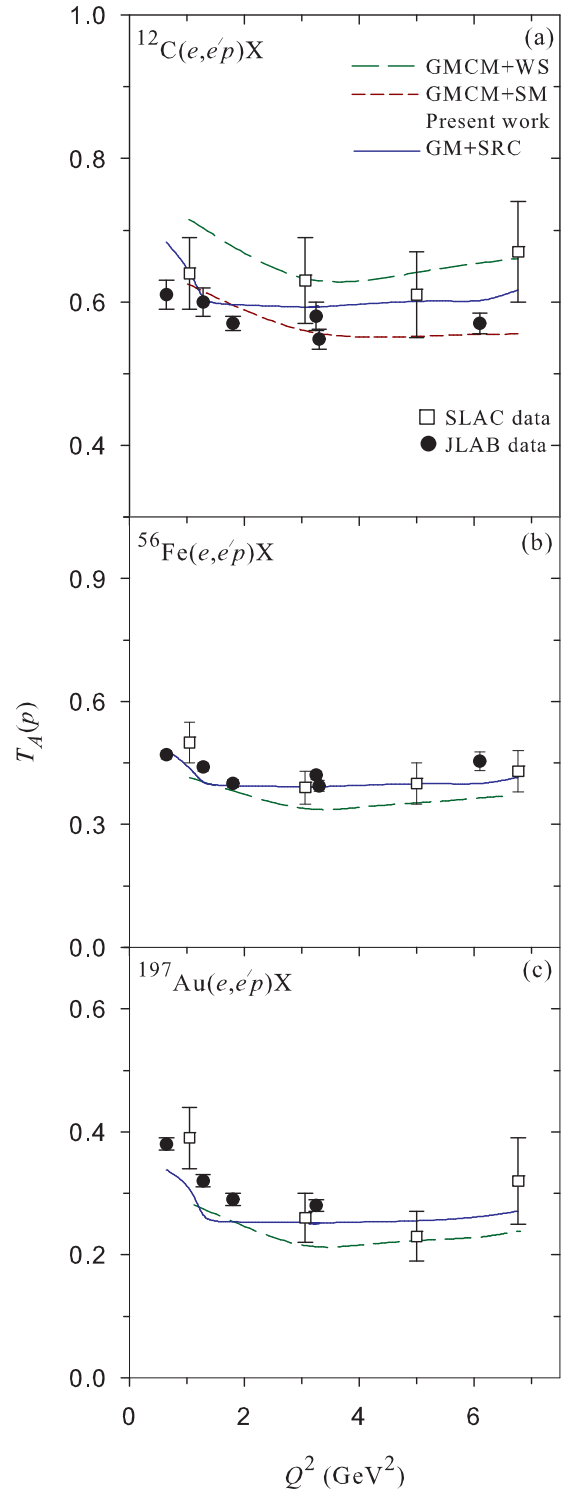


FIG. 2. The proton transparency $T_A(p)$ calculated by Frankel *et al.* [14] using Glauber Monte Carlo method (GMCM). The density of nuclei is accounted by Woods-Saxon (WS) and that also is done by shell-model (SM) for $^{12}$C only. The long-dashed and short-dashed curves arise because of GMCM + WS and GMCM + SM respectively. Those results are compared with $T_A(p)$ due to GM + SRC (solid curves) in the present work described in Fig. 1. The data are taken from Refs. [11,12].

the nucleus. The SRC arises because of the repulsive (short-range) interaction between the nucleons bound in a nucleus. This interaction keeps the bound nucleons apart ($\approx$ 1 fm), which is called nuclear granularity [8]. Therefore, the SRC prevents the shadowing of the hadron-nucleon interaction due to the surrounding nucleons present in a nucleus. This occurrence, as elucidated by Glauber model [5], leads to the enhancement in $\sigma_{hA}$. The SRC is widely used to investigate various aspects in nuclear physics [26].

## II. FORMALISM

A hadron $h$ is produced in the $A(e,e')X$ reaction because of the interaction of the virtual photon $\gamma^*$ (emitted at the $ee'$ vertex) with the nucleus $A$. In this reaction, the nucleus in the final state denoted by $X$ is unspecified. The scattering amplitude for the $\gamma^*A \to hX$ transition, according to Glauber model [1], can be written as

$$F_{X0}[(\mathbf{q}-\mathbf{k}_h)_\perp] = \frac{iq}{2\pi}\int d\mathbf{b}\, e^{i(\mathbf{q}-\mathbf{k}_h)_\perp\cdot\mathbf{b}}\Gamma^{\gamma^*h}_{X0}(\mathbf{b}), \tag{3}$$

where $\mathbf{q}$ and $\mathbf{k}_h$ are the momenta of $\gamma^*$ and $h$ respectively. $\Gamma^{\gamma^*h}_{X0}(\mathbf{b})$ describes the matrix element for the transition of the nucleus from its initial to final states, i.e.,

$$\Gamma^{\gamma^*h}_{X0}(\mathbf{b}) = \langle X|\Gamma^{\gamma^*h}_{A}(\mathbf{b},\mathbf{r}_1,\ldots,\mathbf{r}_A)|0\rangle, \tag{4}$$

where $|0\rangle$ denotes the ground state of the target nucleus and $|X\rangle$ represents the unspecified nuclear state in the exit channel. The nuclear profile operator $\Gamma^{\gamma^*h}_{A}(\mathbf{b},\mathbf{r}_1,\ldots,\mathbf{r}_A)$ [1,27] is given by

$$\Gamma^{\gamma^*h}_{A}(\mathbf{b},\mathbf{r}_1,\ldots,\mathbf{r}_A) = \sum_i \Gamma^{\gamma^*h}(\mathbf{b}-\mathbf{b}_i)e^{i(\mathbf{q}-\mathbf{k}_h)_\parallel z_i} \times \prod_{j\neq i}^{A-1}[1-\Gamma^{hN}(\mathbf{b}-\mathbf{b}_j)\theta(z_j-z_i)]. \tag{5}$$

The summation $i$ is taken over the number of nucleons in the nucleus participating in the hadron production, e.g., the protons in the nucleus taking part to produce the charged hadrons in the reaction.

$\Gamma^{\gamma^*h}(\tilde{\mathbf{b}})$ is the two-body profile function for the hadron produced from the nucleon, i.e., $\gamma^*N \to hN$ process. It is related to the reaction amplitude $f_{\gamma^*h}(\tilde{\mathbf{q}}_\perp)$ [1] as

$$\Gamma^{\gamma^*h}(\tilde{\mathbf{b}}) = \frac{1}{i2\pi q}\int d\tilde{\mathbf{q}}_\perp e^{-i\tilde{\mathbf{q}}_\perp\cdot\tilde{\mathbf{b}}} f_{\gamma^*h}(\tilde{\mathbf{q}}_\perp). \tag{6}$$

The two-body profile function $\Gamma^{hN}(\tilde{\mathbf{b}})$ is connected to $hN$ (hadron-nucleon) elastic scattering amplitude $f_{hN}(\tilde{\mathbf{q}}_\perp)$ [1,5] as

$$f_{hN}(\tilde{\mathbf{q}}'_\perp) = \frac{ik_h}{2\pi}\int d\tilde{\mathbf{b}}' e^{i\tilde{\mathbf{q}}'_\perp\cdot\tilde{\mathbf{b}}'}\Gamma^{hN}(\tilde{\mathbf{b}}'). \tag{7}$$

The nuclear states, assuming the independent particle model [28], can be written in terms of the single-particle state $\Phi$ as $|0\rangle = \prod_{l=1}^{A}|\Phi_0(\mathbf{r}_l)\rangle$ and $|X\rangle = |\Phi_X(\mathbf{r}_m)\rangle\prod_{n\neq m}^{A-1}|\Phi_0(\mathbf{r}_n)\rangle$. Using those, $\Gamma^{\gamma^*h}_{X0}(\mathbf{b})$ in Eq. (4) can be written as

$$\Gamma^{\gamma^*h}_{X0}(\mathbf{b}) = \sum_i \int d\mathbf{r}_i\Phi^*_X(\mathbf{r}_i)\Gamma^{\gamma^*h}(\mathbf{b}-\mathbf{b}_i)e^{i(\mathbf{q}-\mathbf{k}_h)_\parallel z_i} \times \Phi_0(\mathbf{r}_i)D(\mathbf{b},z_i), \tag{8}$$

where $D(\mathbf{b},z_i)$ is given by

$$\begin{aligned} D(\mathbf{b},z_i) &= \prod_{j\neq i}^{A-1}\int d\mathbf{r}_j\Phi^*_0(\mathbf{r}_j)[1-\Gamma^{hN}(\mathbf{b}-\mathbf{b}_j)\theta(z_j-z_i)] \times \Phi_0(\mathbf{r}_j) \\ &= \left[1-\frac{1}{A}\int d\mathbf{b}_j\Gamma^{hN}(\mathbf{b}-\mathbf{b}_j) \times \int dz_j\theta(z_j-z_i)\varrho(\mathbf{r}_j)\right]^{A-1}. \end{aligned} \tag{9}$$

$\varrho(\mathbf{r}_j)$ in the above equation is the matter density distribution of the nucleus, i.e., $\varrho(\mathbf{r}_j) = A|\Phi_0(\mathbf{r}_j)|^2$. $\varrho(\mathbf{b}_j,z_j)$ can be replaced by $\varrho(\mathbf{b},z_j)$ since $\Gamma^{hN}(\mathbf{b}-\mathbf{b}_j)$ varies much more rapidly than $\varrho(\mathbf{b}_j,z_j)$ [1]. Using Eq. (7) and $\mathcal{L}t_{n\to\infty}(1+\frac{x}{n})^n = e^x$, the above equation can be simplified to

$$D(\mathbf{b},z_i) \simeq e^{-\frac{1}{2}\sigma_t^{hN}[1-i\alpha_{hN}]T(\mathbf{b},z_i)}, \tag{10}$$

where $\alpha_{hN}$ denotes the ratio of the real to imaginary parts of the hadron-nucleon scattering amplitude $f_{hN}(0)$, and $\sigma_t^{hN} = \frac{4\pi}{k_h}Im[f_{hN}(0)]$ is the hadron-nucleon total cross section. $T(\mathbf{b},z_i)$ is the partial thickness function of the nucleus, i.e.,

$$T(\mathbf{b},z_i) = \int_{z_i}^{\infty} dz_j\varrho(\mathbf{b},z_j). \tag{11}$$

Using Eq. (8), $F_{X0}[(\mathbf{q}-\mathbf{k}_h)_\perp]$ in Eq. (3) can be expressed as

$$\begin{aligned} F_{X0} &= \frac{iq}{2\pi}\int d\mathbf{b}\, e^{i(\mathbf{q}-\mathbf{k}_h)_\perp\cdot\mathbf{b}}\sum_i\int d\mathbf{r}_i\Phi^*_X(\mathbf{r}_i) \times \Gamma^{\gamma^*h}(\mathbf{b}-\mathbf{b}_i)e^{i(\mathbf{q}-\mathbf{k}_h)_\parallel z_i}\Phi_0(\mathbf{r}_i)D(\mathbf{b},z_i), \\ &= \sum_i\int d\mathbf{r}_i\Phi^*_X(\mathbf{r}_i)f^{(i)}_{hN}([\mathbf{q}-\mathbf{k}_h]_\perp)e^{i(\mathbf{q}-\mathbf{k}_h)\cdot\mathbf{r}_i}\Phi_0(\mathbf{r}_i)D(\mathbf{r}_i), \end{aligned} \tag{12}$$

where $f^{(i)}_{hN}$, defined in Eq. (7), can be considered identically equal for all nucleons.

## III. RESULT AND DISCUSSIONS

The nuclear transparency $T_A$ of the hadron produced in the A$(e,e')$X reaction has been calculated to describe its dependence on the photon virtuality $Q^2$ in the multi-GeV region. The nucleus in the final state $|X\rangle$ differs from its initial state $|0\rangle$ (i.e., ground state) for charged hadron production, i.e., $\Phi_X \neq \Phi_0$ and $F_{00} = 0$. To calculate the cross section, $|F_{X0}|^2$ is multiplied by the phase-space of the reaction and that is divided by the incident flux. Since the final state $|X\rangle$ of the nucleus is not detected, the summation over all states has to be carried out. In the multi-GeV region, the phase space

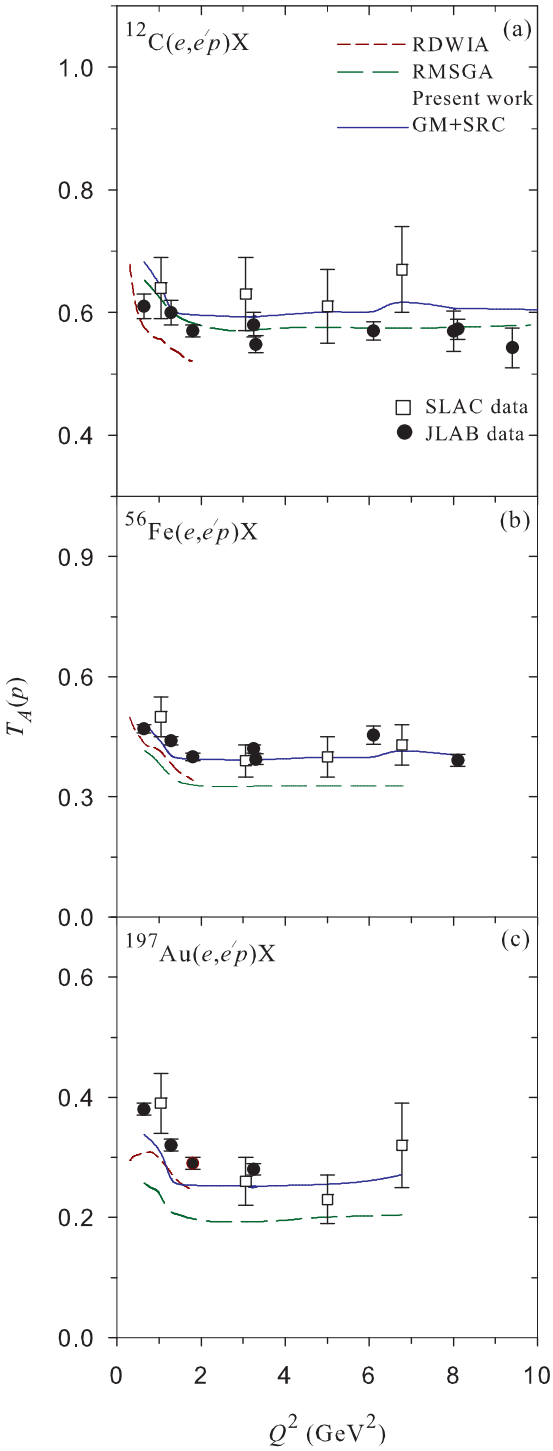


FIG. 3. The short-dashed and long-dashed curves refer to the calculated proton transparency $T_A(p)$, as shown by Lava *et al.* [15], due to the relativistic distorted wave approximation (RDWIA) and relativistic multiple-scattering Glauber approximation (RMSGA) respectively. The solid curves due to GM + SRC in the present work (as illustrated in Fig. 1) are shown for comparison. The data are taken from Refs. [11–13].

of the reaction can be considered independent of the state $|X\rangle$, and therefore the nuclear transparency $T_A$ can be written [1] as

$$T_A = \frac{\sum_{X\neq 0} |F_{X0}|^2}{\sum_{X\neq 0} |F_{X0}|^2_{\rm PWIA}}. \tag{13}$$

The hadron-nucleon cross section $\sigma_t^{hN}$ in free space is used in Eq. (10) to evaluate $T_A$ in the Glauber model. To look for the color transparency (CT), $\sigma_t^{hN}$ (according to the quantum diffusion model [2,21]) has to be replaced by $\sigma_{t,CT}^{hN}$:

$$\sigma_{t,CT}^{hN}(Q^2, l_z) = \sigma_t^{hN}\left[\left\{\frac{l_z}{l_h} + \frac{n_q^2\langle k_t^2\rangle}{Q^2}\left(1 - \frac{l_z}{l_h}\right)\right\} \times \theta(l_h - l_z) + \theta(l_z - l_h)\right], \tag{14}$$

where $Q^2$ is the spacelike four-momentum transfer, i.e., photon virtuality. $n_q$ denotes the number of valence quarks and/or antiquarks present in the hadron, e.g., $n_q = 2$ (3) for a pion (proton) [2]. $k_t$ illustrates the transverse momentum of the (anti)quark: $\langle k_t^2\rangle^{1/2} = 0.35$ GeV/$c$. $l_z$ is the path length traversed by the hadron after its production. The hadron formation length $l_h$ ($\propto \frac{1}{\Delta M^2}$) is already defined in Eq. (2).

The short-range correlation (SRC) can be incorporated by replacing the nuclear density distribution $\varrho$ in Eq. (11) by

$$\varrho(\mathbf{b}, z_j) \to \varrho(\mathbf{b}, z_j)C(|z_j - z_i|), \tag{15}$$

where $C(u)$ represents the correlation function [8]. Using the nuclear matter estimate, it can be written as

$$C(u) = \left[1 - \frac{h(u)^2}{4}\right]^{1/2}[1 + f(u)], \tag{16}$$

with $h(u) = 3\frac{j_1(k_F u)}{k_F u}$ and $f(u) = -e^{-\alpha u^2}(1 - \beta u^2)$. The Fermi momentum $k_F$ is chosen equal to 1.36 fm$^{-1}$. $C(u)$ with the parameters $\alpha = 1.1$ fm$^{-2}$ and $\beta = 0.68$ fm$^{-2}$ agrees well that derived from many-body calculations [8].

The nuclear transparency $T_A$ of the charged hadron, i.e., proton and $\pi^+$ meson, produced in the semi-inclusive electronuclear reaction has been calculated using the Glauber model (GM), where the measured nuclear density distribution $\varrho(r)$ [29] and hadron-nucleon cross section $\sigma_t^{hN}$ [30] are used. As shown later in Figs. 1 and 4, the calculated results due to the GM (presented by the medium-dashed curves) underestimate the measured $T_A$ for both proton and pion. Therefore, the GM has been modified by taking account of the CT and SRC. The dot-dot-dashed and dot-dashed curves denote the calculated $T_A$ due to the incorporation of the CT in the GM for $\Delta M^2$, defined in Eq. (2), taken equal to 0.7 and 1.4 GeV$^2$ respectively. The calculated results increase with $Q^2$ because the CT depends on the energy. $T_A$ evaluated due to the SRC included in GM are presented by the solid curves. They do not show $Q^2$ dependence since the SRC (unlike CT) is independent of energy.

The proton transparency $T_A(p)$ in the $A(e, e'p)X$ reaction has been calculated using the CT of the proton ($p$CT) in the Glauber model (GM + $p$CT) for $^{12}$C, $^{56}$Fe, and $^{197}$Au nuclei. The calculated results vs $Q^2$ are compared in Fig. 1 with the data reported from SLAC [11] (white squares) and JLab [12,13] (black circles). Figure 1(a) shows that the CT does not exist for the proton moving through $^{12}$C for a wide range of $Q^2$, i.e., 0.64–14.2 GeV$^2$. This is corroborated by

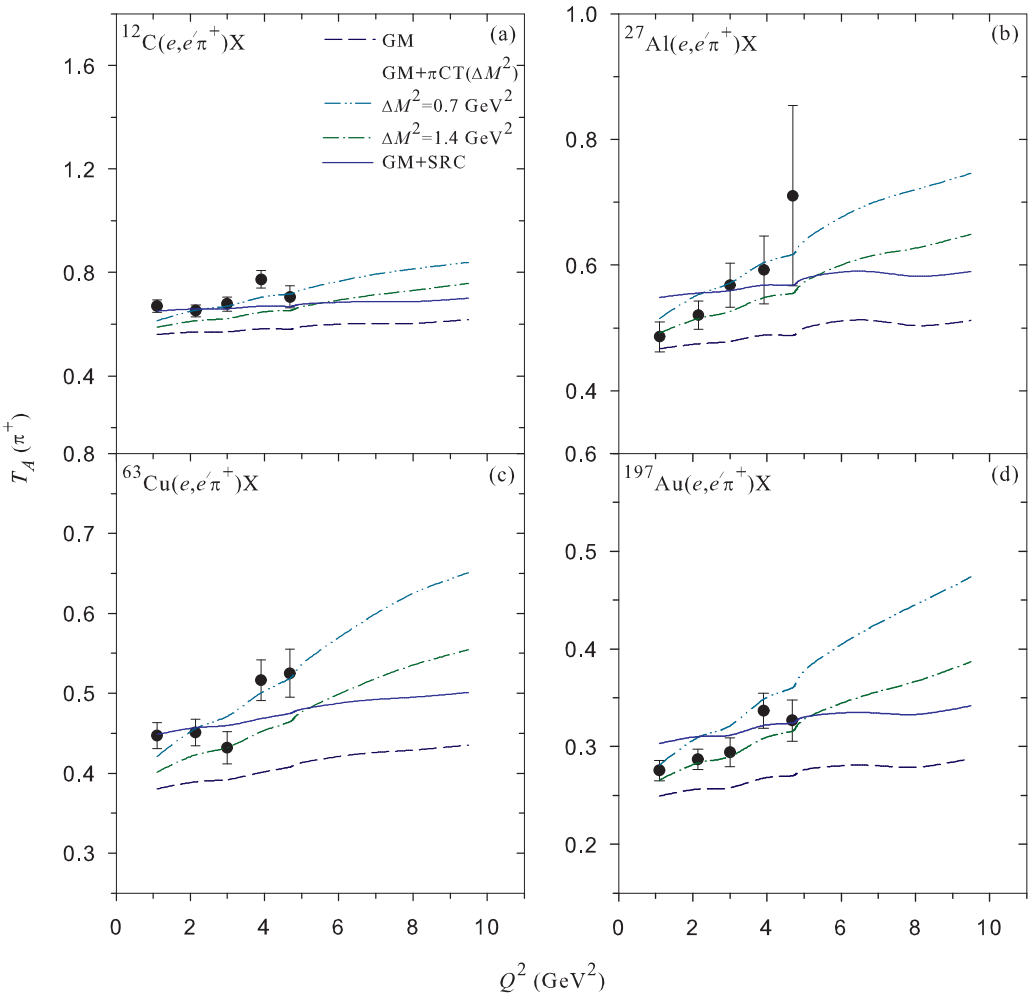


FIG. 4. As in Fig. 1 but for the pionic transparency $T_A(\pi^+)$. The data are taken from Ref. [20].

the results for other nuclei shown in Figs. 1(b) and 1(c), where the data are available for lesser ranges of $Q^2$, i.e., $0.64 \leqslant Q^2 \leqslant 8.1$ GeV$^2$ for $^{56}$Fe and $0.64 \leqslant Q^2 \leqslant 6.77$ GeV$^2$ for $^{197}$Au. Fig. 1 also shows that the calculated $T_A(p)$ due to the inclusion of the SRC in the Glauber model (GM + SRC) reproduce the data reasonably well for all nuclei.

There exist calculations where the $p$CT is not considered to evaluate $T_A(p)$ in the $A(e, e'p)X$ reaction. For example, Frankel *et al.* [14] have calculated $T_A(p)$ using the Glauber Monte Carlo method (GMCM) in which Jastrow-type spatial correlation is included. The density of the C, Fe, and Au nuclei is described by Woods-Saxon (WS) single-particle density. They have also calculated $T_A(p)$, only for the $^{12}$C nucleus, using the nuclear density determined by filled $0s_{1/2}$-$0p_{3/2}$ shell-model (SM) wave functions. The calculated results are shown in Fig. 2, where the long-dashed curves arise due to GMCM + WS and the short-dashed curves occur because of GMCM + SM. Lava *et al.* [15] have shown $T_A(p)$ evaluated using the relativistic distorted-wave impulse approximation (RDWIA) and relativistic multiple-scattering Glauber approximation (RMSGA). The final state interactions treated in those approaches differ from each other. As mentioned in Ref. [15], the SRC of nucleons has been let out and the calculated $T_A(p)$ for $^{208}$Pb is compared to $^{197}$Au data. The results due to RDWIA (short-dashed curves) and RMSGA (long-dashed curves) are presented in Fig. 3. The above mentioned calculated results are compared with $T_A(p)$ due to GM + SRC (solid curves in Figs. 2 and 3) in the present work, as explained in Fig. 1. The data are taken from Refs. [11–13].

The pionic transparency $T_A(\pi^+)$ for $Q^2 = 1.1$–$4.69$ GeV$^2$ in the $A(e, e'\pi^+)X$ reaction was measured at JLab [20] for $^{12}$C, $^{27}$Al, $^{63}$Cu, and $^{197}$Au nuclei to search for the color transparency of the pion ($\pi$CT). The data for all nuclei (except $^{12}$C) show the enhancement of $T_A(\pi^+)$ with $Q^2$. There are proposals to measure $T_A(\pi^+)$ at JLab for higher $Q^2$, i.e., $5 \leqslant Q^2 \leqslant 9.5$ GeV$^2$ [3,31]. Therefore, $T_A(\pi^+)$ for $Q^2 = 1.1$–$9.5$ GeV$^2$ have been calculated and they are presented in Fig. 4 along with the data available from JLab [20]. The calculated results due to the $\pi$CT included in Glauber model (GM + $\pi$CT) are in accord with both the $Q^2$ dependence and magnitude of the data. $T_A(\pi^+)$ estimated incorporating the SRC in the Glauber model (GM + SRC) do not describe the $Q^2$ dependence of the data but they agree with a large number of data points within the errors. Therefore, the data of $T_A(\pi^+)$ in the region

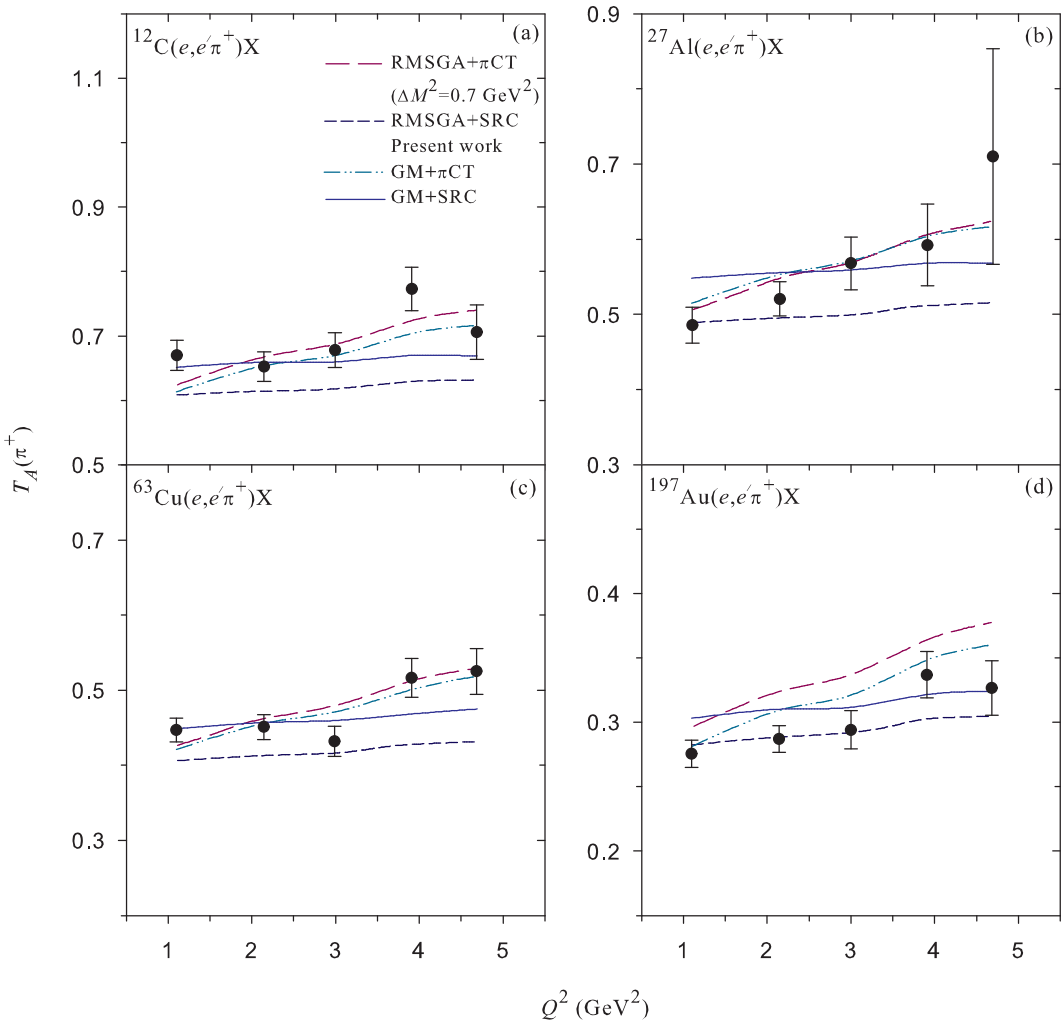


FIG. 5. The pionic transparency $T_A(\pi^+)$ calculated by Cosyn *et al.* [22] using the relativistic multiple-scattering Glauber approach (RMSGA). The effects of pionic color transparency ($\pi$CT) for $\Delta M^2 = 0.7$ GeV$^2$ and short-range correlation (SRC) included in RMSGA are described by the long-dashed curves (RMSGA + $\pi$CT) and short-dashed curves (RMSGA + SRC) respectively. Those results are compared with $T_A(\pi^+)$ due to GM + $\pi$CT (dot-dot-dashed curves) and GM + SRC (solid curves) in the present work; see Fig. 4. The data are taken from Ref. [20].

of $Q^2 = 5$–$9.5$ GeV$^2$ are necessary to prove the existence of $\pi$CT.

The effects of $\pi$CT (for $\Delta M^2 = 0.7$ GeV$^2$) and SRC (Jastrow type) on $T_A(\pi^+)$ in the $A(e, e'\pi^+)X$ reaction have also been discussed by Cosyn *et al.* [22] in their calculation based on the relativistic multiple-scattering Glauber approximation (RMSGA). In Fig. 5, the calculated results due to RMSGA + $\pi$CT and RMSGA + SRC are denoted by the long-dashed and short-dashed curves respectively. Kaskulov *et al.* [23] have studied $T_A(\pi^+)$ in the above reaction using the couple-channels (CC) treatment for the pion-nucleus interaction, and discussed the effects of pion production mechanisms in the elementary $(\gamma^*, \pi^+)$ reaction. However, they have not considered the SRC of nucleons. Among the calculated results [23], $T_A(\pi^+)$ evaluated using the Lund model (LM) for the pion formation time (dilated) along with the pedestal value of the pion-nucleon effective cross section ($Q^2$ independent) provide a good description of the data. The calculated results due to CC + LM are denoted by the long-dashed curves in Fig. 6. Other curves in Figs. 5 and 6 due to present work (see Fig. 4) are shown for comparison. The data are taken from Ref. [20].

## IV. CONCLUSIONS

The nuclear transparencies $T_A$ of the proton and $\pi^+$ meson produced in the $(e, e')$ reaction on nuclei have been calculated using the Glauber model for a wide range of photon virtuality $Q^2$. $T_A$ estimated using the Glauber model do not reproduce the measured transparencies for both proton and pion. To realize the data, $T_A$ is calculated incorporating the color transparency of the produced hadron and the short-range correlation of the bound nucleon in the Glauber model. The calculated results for the proton and pion are compared with the data. The transparency of the proton $T_A(p)$ evaluated using color transparency in the Glauber model does not reproduce

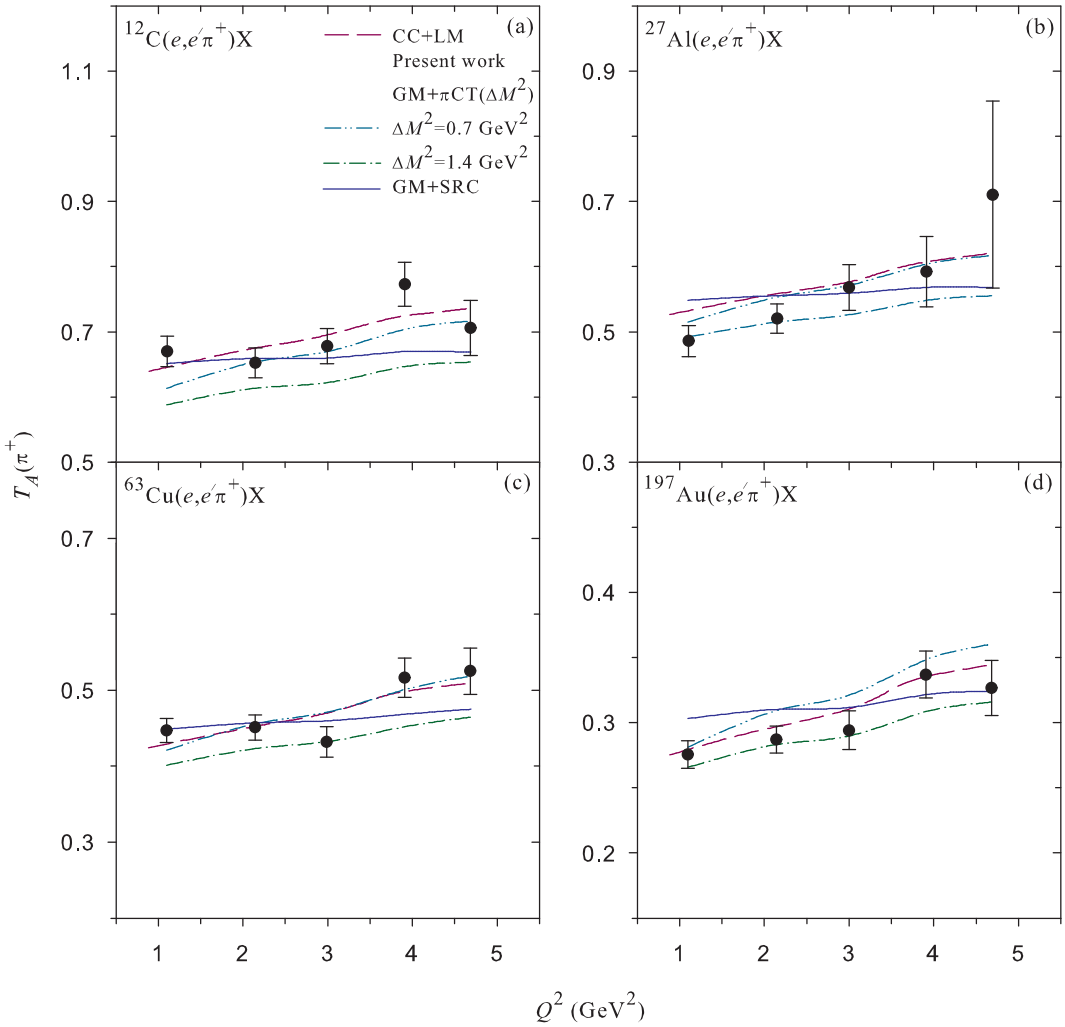


FIG. 6. The transparency $T_A(\pi^+)$ calculated by Kaskulaov *et al.*, [23] based on Lund model (LM) and couple-channel (CC) approach, see text. The long-dashed curves represent the calculated results due to CC + LM. Other curves occurred due to the present work (see Fig. 4) have been shown for comparison. The data are taken from Ref. [20].

the data, where as the calculated $T_A(p)$ due to the short-range correlation added in the Glauber model accords well with the data. The calculated transparency of the pion $T_A(\pi^+)$ considering the color transparency in the Glauber model agrees with both the $Q^2$ dependence and magnitude of the data, available for $1.1 \leqslant Q^2 \leqslant 4.69$ GeV$^2$. The calculated $T_A(\pi^+)$ due to the inclusion of the short-range correlation in the Glauber model agree with a large number of data points within the errors, but those do not explain the $Q^2$ dependence of the measured spectra. Therefore, $T_A(\pi^+)$ for $Q^2 = 5$–$9.5$ GeV$^2$, to be measured at JLab, are required to confirm the pionic color transparency.

## ACKNOWLEDGMENTS

The author appreciates the anonymous referee for comments which improved the quality of the work. The author is grateful to Dipangkar Dutta for the discussions on experimental results, and thanks A. K. Gupta and S. M. Yusuf for their encouragement to work on theoretical nuclear physics.

[1] G. T. Howell and G. A. Miller, Phys. Rev. C **88**, 035202 (2013).
[2] G. R. Farrar, H. Liu, L. L. Frankfurt, and M. I. Strikman, Phys. Rev. Lett. **61**, 686 (1988).
[3] D. Dutta, K. Hafidi, and M. Strikman, Prog. Part. Nucl. Phys. **69**, 1 (2013).
[4] A. B. Larionov, M. Strikman, and M. Bleicher, Phys. Rev. C **93**, 034618 (2016).
[5] R. J. Glauber, in *Lectures in Theoretical Physics*, edited by W. E. Brittin *et al.* (Interscience, New York, 1959), Vol. I, p. 315; J. M. Eisenberg and D. S. Kolton, *Theory of Meson Interaction with Nuclei* (John Wiley & Sons, New York, 1980), p. 158.
[6] L. L. Frankfurt, G. A. Miller, and M. Strikman, Annu. Rev. Nucl. Part. Sci. **44**, 501 (1994); L. Frankfurt and M. Strikman, Phys. Rep. **160**, 235 (1988); P. Jain, B. Pire, and J. P. Ralston, *ibid.* **271**, 67 (1996).

[7] A. S. Carroll, D. S. Barton, G. Bunce, S. Gushue, Y. I. Makdisi, S. Heppelmann, H. Courant, G. Fang, K. J. Heller, M. L. Marshak, M. A. Shupe, and J. J. Russell, Phys. Rev. Lett. **61**, 1698 (1988); I. Mardor, S. Durrant, J. Aclander, J. Alster, D. Barton, G. Bunce, A. Carroll, N. Christensen, H. Courant, S. Gushue, S. Heppelmann, E. Kosonovsky, Y. Mardor, M. Marshak, Y. Makdisi, E. D. Minor, I. Navon, H. Nicholson, E. Piasetzky, T. Roser *et al.*, *ibid.* **81**, 5085 (1998); A. Leksanov, J. Alster, G. Asryan, Y. Averichev, D. Barton, V. Baturin, N. Bukhtoyarova, A. Carroll, S. Heppelmann, T. Kawabata, Y. Makdisi, A. Malki, E. Minina, I. Navon, H. Nicholson, A. Ogawa, Y. Panebratsev, E. Piasetzky, A. Schetkovsky, S. Shimanskiy *et al.*, *ibid.* **87**, 212301 (2001); J. Aclander, J. Alster, G. Asryan, Y. Averiche, D. S. Barton, V. Baturin, N. Buktoyarova, G. Bunce, A. S. Carroll, N. Christensen, H. Courant, S. Durrant, G. Fang, K. Gabriel, S. Gushue, K. J. Heller, S. Heppelmann, I. Kosonovsky, A. Leksanov, Y. I. Makdisi, A. Malki *et al.*, Phys. Rev. C **70**, 015208 (2004).

[8] T.-S. H. Lee and G. A. Miller, Phys. Rev. C **45**, 1863 (1992).

[9] S. J. Brodsky and G. F. de Teramond, Phys. Rev. Lett. **60**, 1924 (1988).

[10] J. P. Ralston and B. Pire, Phys. Rev. Lett. **61**, 1823 (1988).

[11] T. G. O'Neill *et al.*, Phys. Lett. B **351**, 87 (1995); N. C. R. Makins, R. Ent, M. S. Chapman, J. O. Hansen, K. Lee, R. G. Milner, J. Nelson, R. G. Arnold, P. E. Bosted, C. E. Keppel, A. Lung, S. E. Rock, M. Spengos, Z. M. Szalata, L. H. Tao, J. L. White, K. P. Coulter, D. F. Geesaman, R. J. Holt, H. E. Jackson *et al.*, Phys. Rev. Lett. **72**, 1986 (1994).

[12] D. Dutta *et al.*, Phys. Rev. C **68**, 064603 (2003); D. Abbott *et al.*, Phys. Rev. Lett. **80**, 5072 (1998); K. Garrow *et al.*, Phys. Rev. C **66**, 044613 (2002).

[13] D. Bhetuwal *et al.*, Phys. Rev. Lett. **126**, 082301 (2021).

[14] S. Frankel, W. Frati, and N. R. Walet, Phys. Rev. C **51**, R1616 (1995).

[15] P. Lava, M. C. Martínez, J. Rychebusch, J. A. Caballero, and J. M. Udías, Phys. Lett. B **595**, 177 (2004).

[16] E. M. Aitala *et al.*, Phys. Rev. Lett. **86**, 4773 (2001).

[17] D. Dutta *et al.* (Jefferson Lab E94104 Collaboration), Phys. Rev. C **68**, 021001R (2003).

[18] A. Airapetian *et al.*, Phys. Rev. Lett. **90**, 052501 (2003); L. El Fassi *et al.*, Phys. Lett. B **712**, 326 (2012).

[19] B. Z. Kopeliovich, J. Nemchik, and I. Schmidt, Phys. Rev. C **76**, 015205 (2007); L. Frankfurt, G. A. Miller, and M. Strikman, *ibid.* **78**, 015208 (2008); K. Gallmeister, M. Kaskulov, and U. Mosel, *ibid.* **83**, 015201 (2011).

[20] B. Clasie *et al.*, Phys. Rev. Lett. **99**, 242502 (2007); X. Qian *et al.*, Phys. Rev. C **81**, 055209 (2010).

[21] A. Larson, G. A. Miller, and M. Strikman, Phys. Rev. C **74**, 018201 (2006).

[22] W. Cosyn, M. C. Martínez, and J. Ryckebusch, Phys. Rev. C **77**, 034602 (2008).

[23] M. M. Kaskulov, K. Gallmeister, and U. Mosel, Phys. Rev. C **79**, 015207 (2009).

[24] S. Kumano, J. Phys.: Conf. Ser. **312**, 032005 (2011); Int. J. Mod. Phys. Conf. Ser. **40**, 1660009 (2016).

[25] G. A. Miller and M. Strikman, Phys. Rev. C **82**, 025205 (2010).

[26] G. A. Miller and J. E. Spencer, Ann. Phys. (NY) **100**, 562 (1976); O. Benhar, A. Fabrocini, S. Fantoni, G. A. Miller, V. R. Pandharipande, and I. Sick, Phys. Rev. C **44**, 2328 (1991); S. Das, Phys. Scr. **96**, 035304 (2021).

[27] J. Hüfner, B. Kopeliovich, and J. Nemchik, Phys. Lett. B **383**, 362 (1996).

[28] T. H. Bauer, R. D. Spital, D. R. Yennie, and F. M. Pipkin, Rev. Mod. Phys. **50**, 261 (1978); **51**, 407(E) (1979).

[29] C. W. De Jager, H. De Vries, and C. De Vries, At. Data Nucl. Data Tables **14**, 479 (1974); **36**, 495 (1987).

[30] P. A. Zyla *et al.* (Particle Data Group), Prog. Theor. Exp. Phys. **2020**, 083C01 (2020); https://pdg.lbl.gov/2020/hadronic-xsections/hadron.html; C. Lechanoine-Leluc and F. Lehar, Rev. Mod. Phys. **65**, 47 (1993); D. V. Bugg *et al.*, Phys. Rev. **146**, 980 (1966); S. Barshay, C. B. Dover, and J. P. Vary, Phys. Rev. C **11**, 360 (1975).

[31] D. Dutta (private communication).